ELSEVIER

Journal of Alloys and Compounds 330–332 (2002) 202–207

Journal of ALLOYS AND COMPOUNDS

www.elsevier.com/locate/jallcom

In-situ neutron powder diffraction study of annealing activated $LaNi_5$

E.H. Kisi[a,]*, E. Wu[a], M. Kemali[b]

[a]Department of Mechanical Engineering, The University of Newcastle, Callaghan, NSW 2308, Australia
[b]Department of Physics, The University of Salford, Salford, Greater Manchester M5 4WT, UK

Abstract

In-situ neutron powder diffraction measurements and the Rietveld refinement technique have been used to study a fully hydrogen activated $LaNi_5$ alloy during annealing in the temperature range 293 to 1123 K. Diffraction data were analysed by imposing a dislocation-induced anisotropic line broadening model, to reveal the variation of dislocation density and defect structure as a function of temperature. The activated sample contained predominantly edge dislocations with Burgers vector $a/3\langle -2110\rangle$ on prismatic $\{0-110\}$ slip planes associated with medium to long ranged strain fields ($M\sim 2$–3). A small proportion of dislocations (~10%) with the same Burger vectors on basal {0001} slip planes are also indicated by the refinements. This second type of dislocation appears to be more resistant to annealing than the dislocations on prismatic slip planes. A progressive decrease in dislocation density from $\sim 6\times 10^{11}/\mathrm{cm}^2$ to the limit of the resolution of our measurement ($\lesssim 10^{10}/\mathrm{cm}^2$) was observed between 293 and 973 K. This annealing appears to cause the restoration of the large pressure hysteresis characteristic of unactivated $LaNi_5$. The most significant reduction in dislocation density occurs at ~800 K. In contrast, TGA measurements show the release of trapped hydrogen at ~500 K. The latter feature is associated with an anomaly in the c/a ratio. The results suggest that, in addition to primary defects in the form of dislocations, a different class of defects such as vacancies and small dislocation loops may also exist in hydrogen activated $LaNi_5$. Further, whereas the former are undoubtedly associated with observed changes in the pressure hysteresis during activation, the latter are likely to be the favoured site for hydrogen trapping in activated $LaNi_5$.

Keywords: Hydrogen activated $LaNi_5$ alloy; Annealing; Neutron diffraction; Dislocations; Defects

1. Introduction

The intermetallic compound $LaNi_5$ is one of the most widely studied metal hydride materials because the low room temperature absorption pressures and ease of activation make it suitable for applications in hydrogen storage, purification and as the basis for metal hydride battery alloys. The compound has an initially high hydrogen absorption pressure (~1 MPa at 300 K) leading to large pressure hysteresis during the first absorption/desorption cycle. The absorption pressure and hysteresis are (i) significantly reduced by the initial activation cycle, (ii) are reduced a little further in the next four to five absorption/desorption cycles, but (iii) are restored after annealing [1,2].

It has been suggested that the first activation cycle introduces a large number of microstructural inhomogeneities such as lattice defects, which provide hydrogen diffusion paths with higher transport rates and accommodate part of the lattice mis-match between the α- and β-phases [2–4]. These alter the kinetics and hysteresis respectively. It has long been noted that very strong anisotropic line broadening is present in the X-ray and neutron diffraction patterns of activated $LaNi_5$ [2,5–9]. The ($hk0$) reflections in the diffraction pattern are most broadened and the ($00l$) lines are nearly unbroadened. This has been modelled as microstrain, primarily on the a-axis $\Delta a/a$ [2]. The combined techniques of in-situ measurement of the diffraction profiles and line broadening analysis using the Rietveld refinement method have allowed us to study dislocations in $LaNi_5$ and its hydrides during hydrogen activation and hydrogenation [2,7,8,10]. We have investigated the relationship between lattice defects, and hydrogen absorption behaviour by studying the diffraction peak broadening interpreted on a dislocation-induced line broadening model [2,7,8]. Dislocations with Burgers vector $a/3\langle -2110\rangle$ predominantly on the prismatic $\{0-110\}$ planes, in the random polycrystalline material generate a (hkl) dependence that best fits the data and provides a sound physical meaning for the anisotropic broadening of activated $LaNi_5$ [5,9].

---

*Corresponding author. Tel.: +61-49-21-6213; fax: +61-49-21-6946.
E-mail address: meehk@cc.newcastle.edu.au (E.H. Kisi).

0925-8388/02/$ – see front matter
PII: S0925-8388(01)01582-1

Annealing of activated $LaNi_5$ reverses the changes caused by activation. It restores the hysteresis, removes the line broadening and, by implication, causes large changes in the defect structure [1,2]. Unlike activation, except for the hydrogenation work of Flanagan et al. [1], the annealing process has not been extensively studied. In this work, we report the results of in-situ neutron diffraction experiments and Rietveld refinement analyses of the annealing behaviour of hydrogen activated $LaNi_5$ powder. The study provides information on the dislocation configuration and density, the kinetics of dislocation annihilation, and the correlation between the dislocation density and the hydrogenation properties of annealed $LaNi_5$ reported in Ref. [1].

2. Experimental

The $LaNi_5$ sample (Johnson Matthey) was subjected to five hydriding/dehydriding cycles at room temperature for activation. The activated powder sample was held in a 12 mm diameter vanadium canister and loaded into an evacuated vanadium furnace (10^{-5} Torr) for the in-situ measurement at the Institut Laue–Langevin (ILL), Grenoble, France.

Neutron diffraction data were collected using the instrument D2B. The instrument was operated in high flux mode and patterns were recorded from 0 to 160° (2θ) in 0.05° steps using a neutron wavelength of $\lambda = 1.597$ Å. The diffraction patterns were collected in repeated scans of 20 min duration for various holding times ranging from 7 h (low temperature) to 2.5 h (high temperature) at 273, 373, 423, 473, 523, 573, 628, 653, 748, 823, 873, 923, 973 and 1123 K.

Structural and dislocation analysis was conducted by Rietveld refinements using a modified version of the program LHPM [11] implementing a dislocation-induced anisotropic line broadening model [7,12]. The model is based on the theories of Krivoglaz et al. [13] and Wilkens [14], which relate the integral breadth β of the broadened peaks to the dislocation structure of the crystallites by $\beta^2 = \rho\chi f(M) \tan^2\theta$, where ρ is the dislocation density, χ is an orientation factor which accounts for the *hkl* dependence of the broadening due to the preferred slip system(s) on which the dislocations lie, $f(M)$ is a function of the dimensionless dislocation distribution parameter M which is given by $M = r\rho^{1/2}$ (where r is the outer cut-off radius of the dislocation strain field) and related to the range of the dislocation strain field [12]. When a specific dislocation slip system is assigned, the program calculates χ, and determines the associated broadening for each reflection. The program has been revised to allow for the refinement of more complicated dislocation structures containing a mixture of two slip systems in activated $LaNi_5$ as recently suggested by Cerny et al. [9]. The instrumental broadening determined from an unbroadened reference sample must be taken into account in this type of analysis. In our case, the pattern from $LaNi_5$ annealed at 1123 K was considered as relatively unbroadened and used as a reference.

A parallel thermogravimetric analysis (TGA) was conducted on a small quantity of the same type of hydrogen activated $LaNi_5$ at Salford University. The temperature was increased from room temperature to 973 K in a vacuum of initially $<1\times10^{-7}$ Torr. Both hydrogen partial pressure and mass change of the sample were monitored during the experiment.

3. Results

Fig. 1 shows the observed changes in the neutron powder diffraction profiles with increasing temperature. The $LaNi_5$ sample in its initial hydrogen activated state

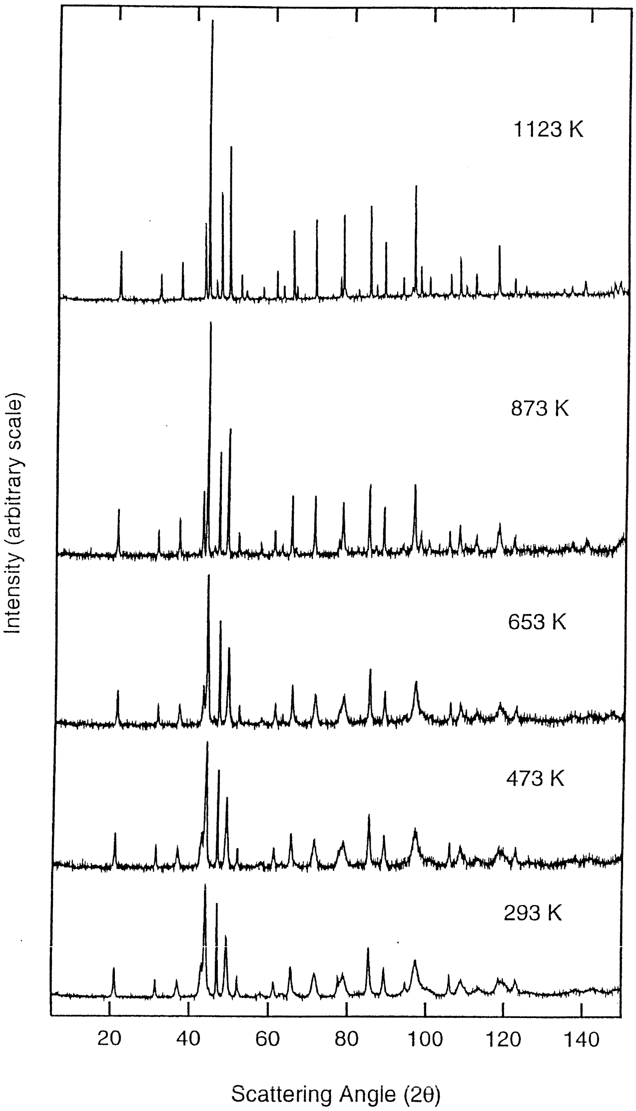

Fig. 1. Neutron diffraction patterns collected at various temperatures during the in-situ annealing experiment showing the reduction in anisotropic broadening.

exhibits very pronounced anisotropic peak broadening which corresponds to a high dislocation density as suggested by our previous work [2,7]. As the annealing temperature is increased, the line broadening is reduced. The most significant decrease occurs at around 800 K, and the line widths become isotropic above 973 K.

A mixed dislocation configuration with Burgers vector $a/3\langle -2110\rangle$ on two types of slip plane, prismatic $\{0-110\}$ and basal $\{0001\}$, was found to give the best agreement with the observed data. The weighted profile R-factor, R_{wp}, was below 5% for all refinements when this mixed dislocation model was applied. Modelling of the dislocation-induced broadening with predominantly $a/3\langle -2110\rangle\{0-110\}$ type dislocations (~90%) is justified by our previous work [7]. The co-existence of $a/3\langle -2110\rangle\{0001\}$ type dislocations (~10%) in the system has recently been determined by Cerny et al. [9] and is also supported by TEM work of Kim et al. [4]. The dislocation density calculated according to this model is plotted in Fig. 2a. The dislocation density in the sample is reduced progressively as the temperature increases from $\sim 6\times10^{11}/\mathrm{cm}^2$ to the limit of the resolution of the fitting technique ($\sim 10^{10}/\mathrm{cm}^2$) between 293 and 973 K in agreement with qualitative observations of the line broadening in Fig. 1. The most significant change in dislocation density occurs at ~800 K. Also shown in Fig. 2b is the sample mass change and gas pressure derived from TGA measurements on the same activated material. These are characterised by a major peak at ~500 K, below the temperature where major changes occur in the dislocation density.

It has previously been reported that the ratio of the lattice parameters, c/a, for activated $LaNi_5$ is larger than that of the unactivated alloy [2,8]. Although the absolute values of the lattice parameters could contain systematic errors, the ratio of the lattice parameters c/a should be relatively stable. In Fig. 2c, the c/a ratio is plotted as a function of annealing temperature. The ratio decreases as the temperature increases showing a pronounced anomaly at around 500 K.

The proportion of the second type of dislocation ($a/3\langle -2110\rangle\{0001\}$) in the mixed dislocation configuration, and the dislocation distribution parameter (M) derived from the Rietveld refinements are shown in Fig. 3. The proportion of the $a/3\langle -2110\rangle\{0001\}$ type dislocation is stable at ~10% at low temperature, but appears to increase moderately (to ~30%) as the temperature increases above 800 K. This is not due to an increase in the number of these dislocations, but rather to their greater stability compared with the $a/3\langle -2110\rangle\{0-110\}$ type dislocations. The dislocation distribution parameter M is fitted at 2–3, and it appears to follow a similar trend with temperature as the proportion of $a/3\langle -2110\rangle\{0001\}$. It should be noted, however, that this parameter became quite unstable and the uncertainty became large at higher temperature due to the smaller amount of broadening.

4. Discussion

Krivoglaz [15] has proposed that there are two classes of defects according to the relative spatial extent of their strain fields. The first class, like small dislocation loops, vacancies, interstitials and small precipitates, are finite defects with a rapidly decreasing strain field, causing changes to the lattice parameters but no line broadening. The second class, like straight dislocations, stacking faults and dislocation cell walls, have essentially infinite length and slowly decreasing strain fields, inducing line broadening but no change to the lattice parameters [15]. The existence of large numbers of the second class of defects in activated $LaNi_5$ has been confirmed by the presence of strong anisotropic line broadening in the diffraction patterns. However, in addition to the line broadening, changes of lattice parameters, mainly reflected in the ratio c/a, are also observed, indicating that there may also be a considerable amount of the first class of defects in the system [9]. The annealing data above contain valuable information on the stability range and influence on hydride formation of both classes of defects.

The significant decrease in the dislocation density during annealing, indicated by the disappearance of the anisotropic broadening at higher temperature (see Fig. 1), correlates very well with the return of the high pressure hysteresis [1]. This strongly supports the theory that the initial creation of large numbers of these defects is the origin of the high absorption pressure and hysteresis in unactivated $LaNi_5$. The principal defect responsible for the severe anisotropic broadening has been verified as straight edge dislocations with Burger's vector $a/3\langle -2110\rangle$ on prismatic slip planes $\{0-110\}$ at an average density of about $6\times10^{11}/\mathrm{cm}^2$ by Rietveld fitting of the diffraction patterns at room temperature. However, by refinement of the data allowing a mixture of two types of dislocation systems, a small proportion of a second type of dislocation with the same Burgers vector $a/3\langle -2110\rangle$ on the basal plane $\{0001\}$ was also revealed. The dislocation distribution parameter M between 2 and 3 indicates that the dislocations in hydrogen cycled $LaNi_5$ are associated with medium to long ranged strain fields with the possibility of slight pile-ups. This dislocation structure is generally consistent with our previous calculation [4,7], and the observation of a second type of dislocation agrees well with Cerny et al. [9]. Due to the relatively inaccurate measurement of the instrumental broadening in the experiment, the dislocation densities calculated in this work are only indicative, providing a relative trend during annealing. The maximum value of $6\times10^{11}/\mathrm{cm}^2$ is lower than our previous calculation from lower resolution data [12], but higher than the value derived by Cerny et al. from synchrotron data [9]. To verify the dislocation density calculated from the method in Ref. [7], we re-examined the work by determining the dislocation density independently

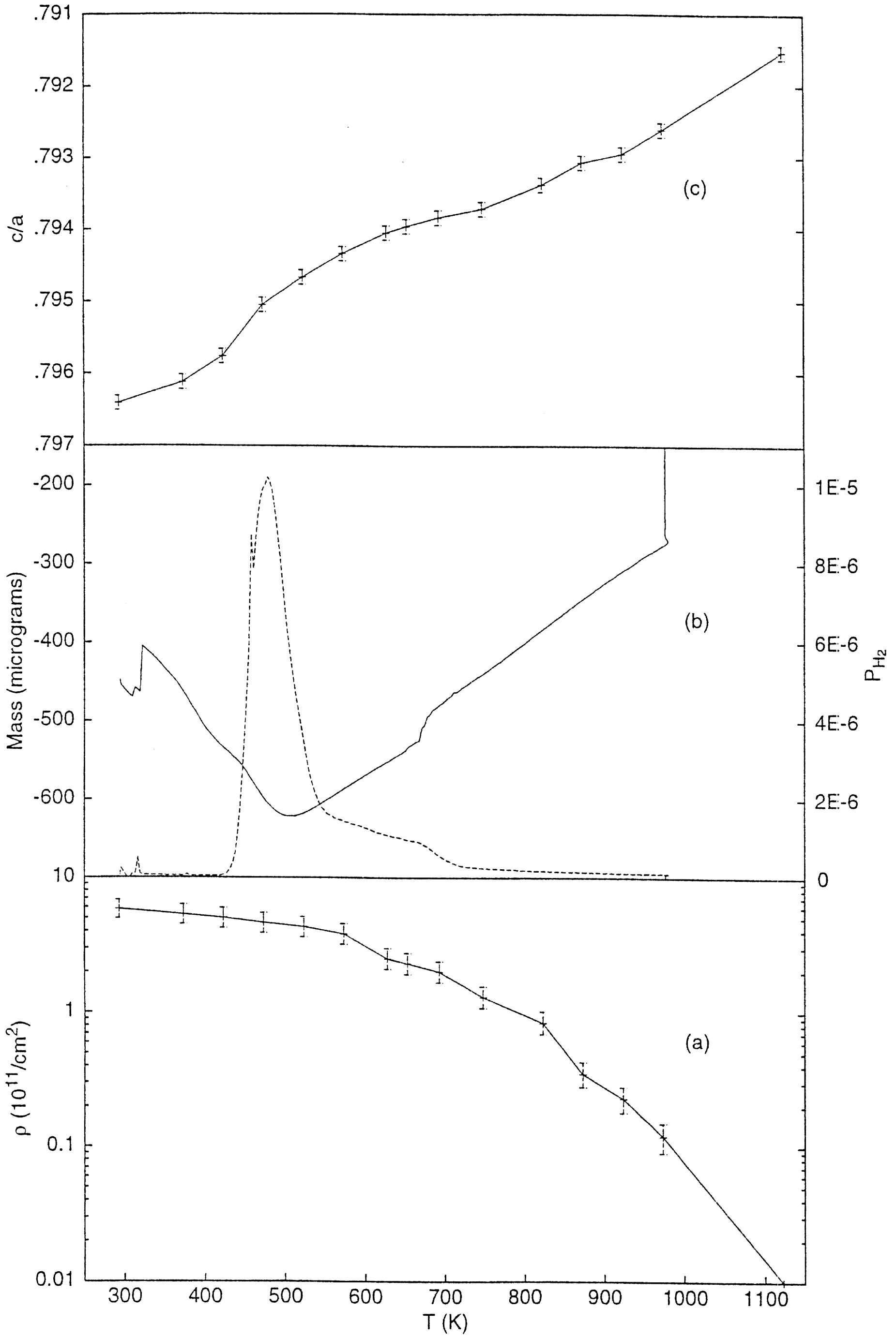

Fig. 2. The change in defect density during annealing as indicated by (a) the dislocation density vs. temperature calculated from line broadening in the neutron diffraction patterns, (b) the sample mass (solid line and left-hand scale) and pressure (dashed line and right-hand scale) derived from TGA and (c) the *c*/*a* ratio vs. temperature derived from Rietveld refinements.

using the method developed by Krivoglaz et al. [13] and by Wilkens [14]. The derived dislocation densities from the two methods differ by only about 1 (in the same order of magnitude) from those reported here. Such high dislocation densities are rarely reported. Other methods of measuring dislocation densities become less accurate at very high dislocation densities, whereas the line broadening method only becomes useable at $>10^9/\mathrm{cm}^2$ (depending on instrument resolution). However, examples of dislocation densities in the same range have appeared in the literature, for example in cyclically deformed copper the dislocation density in macroscopic fatigue bands has been calculated as 10^{11}–$10^{12}/\mathrm{cm}^2$ [16]. The dislocations in activated $LaNi_5$ are caused by interfacial strains be-

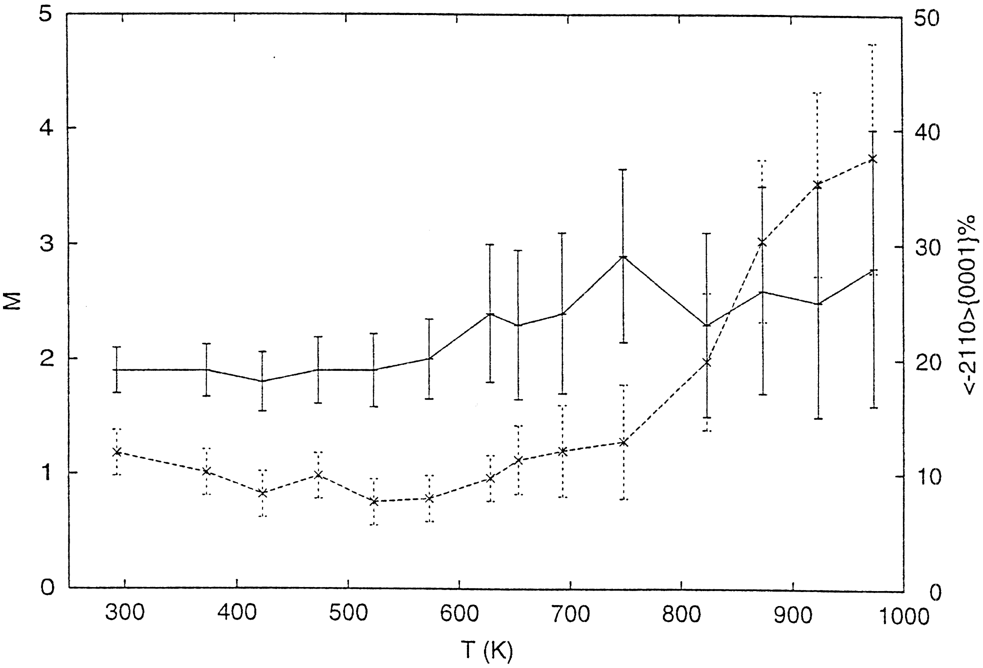

Fig. 3. The proportion of dislocations on the basal plane vs. temperature (dashed line and scale on the right-hand side) and the dislocation distribution parameter *M* vs. temperature (solid line and scale on the left-hand side) derived from the neutron diffraction patterns.

tween the α-phase and the emergent β-phase, which is known to cause severe damage to the alloy. Therefore, the estimated dislocation densities close to $10^{12}/\mathrm{cm}^2$ are not considered unreasonable.

There appear to be several stages to the annealing process — possibly due to different defect annihilation mechanisms. The first stage is from room temperature to about 423 K. In this stage, the dislocation density and structure remain the same (see Figs. 2a and 3). The c/a ratio decreased showing some thermal expansion anisotropy of the $LaNi_5$ lattice (see Fig. 2c). In the same temperature range, there is some mass change in the sample, but no change in hydrogen pressure during the TGA measurement (see Fig. 2b), suggesting the defects in activated $LaNi_5$ are stable in this temperature range.

During the second stage, from 423 to 573 K, there is little change in dislocation density and structure, but a significant change in sample mass associated with a major peak in the hydrogen pressure. This indicates the release of most of the trapped hydrogen in the lattice in this temperature range. Trapped hydrogen in activated $LaNi_5$ has been reported previously, but its causes were not identified. It is interesting to note that the anomaly observed in the c/a ratio (see Fig. 2c) occurs in this same temperature range. These phenomena suggest that the release of the trapped hydrogen is likely to be associated with the loss of defects of the first class like vacancies and dislocation loops, which cause lattice parameter changes but no line broadening effects, rather than the second class of defects (dislocations). These defects are likely to be inherited from the initial formation of α-phase hydride in the first cycle [4], and act as the preferred sites for hydrogen trapping. Once established, trapping sites reduce the amount of hydrogen which may be reversibly stored in $LaNi_5$. These results suggest that the annealing of repeatedly cycled $LaNi_5$ in this temperature range can help to improve the reversibility of hydrogen storage for $LaNi_5$ alloys.

In the third stage, from 573 to 748 K, the lattice parameters, sample mass and hydrogen partial pressure indicate that annihilation of the first class of defects is complete and the line broadening indicates that annihilation of the second class of defects (dislocations) is beginning. Analysis of the line broadening shows a continuous moderate decrease in dislocation density and an accompanying change in the ratio of the two kinds of dislocations (Figs. 2a,b and 3).

The fourth stage occurs from 748 to about 973 K. Here a significant decrease in dislocation density is observed, accompanied by a greater change in the dislocation structure. An increase is observed in the proportion of $a/3\langle -2110\rangle\{0001\}$ type dislocations (from ~10 to ~30%) and a slight change in the M value (from ~2 to ~3). This would appear to indicate that edge dislocations on the basal plane with slightly longer ranged strain field are more resistant to annealing. At higher temperature, little line broadening can be observed visually nor can it be resolved in the Rietveld fitting, indicating that the density of dislocations in the material is well below $10^{10}/\mathrm{cm}^2$, and the hydrogen pressure hysteresis would have been restored in these samples [1]. Therefore, this is a relatively effective annealing temperature range for the annihilation of dislocations in $LaNi_5$.

5. Conclusions

The progressive reduction of strong anisotropic broadening, the change of lattice parameters and the release of trapped hydrogen during the annealing of hydrogen cycled $LaNi_5$ powder at 278 to 1123 K have been observed and are associated with the annihilation of different types of defects in the sample.

At lower temperature (423 to 700 K) anomalous changes of the c/a ratio are associated with the loss of trapped hydrogen observed during TGA. This provides evidence for the existence of defects like vacancies and small dislocation loops which are likely to act as the preferred hydrogen trapping sites in the activated $LaNi_5$ alloy.

The line broadening is associated with a high density of edge dislocations. The predominant dislocation system in cycled $LaNi_5$ is $a/3\langle -2110\rangle\{0-110\}$ with intermediate to long range strain fields. There is an additional small proportion of $a/3\langle -2110\rangle\{0001\}$ type dislocations which appear to have longer ranged strain fields and are more resistant to annealing.

The most significant reduction of anisotropic line broadening occurs at around 800 K, indicating that the annihilation of the second type of defects (the dislocations) at a higher temperature is associated with the restoration of high pressure hysteresis to the $LaNi_5$ alloy.

Acknowledgements

The authors wish to express their thanks to the staff of the Institut Laue–Langevin for their assistance in conducting the experiment. Dr Kisi would also like to acknowledge a French Government Scientific Fellowship.

References

[1] T.B. Flanagan, G.H. Biehl, J. Less-Common Met. 82 (1981) 385.

[2] E.H. Kisi, C.E. Buckley, E.M. Gray, J. Alloys Comp. 185 (1992) 369, and references cited therein.

[3] K. Nomura, H. Uruno, S. Ono, H. Shimozuka, S. Suda, J. Less-Common Met. 107 (1985) 221.

[4] G.-H. Kim, C.-H. Chun, S.-G. Lee, J.-Y. Lee, Acta Metal. Mater. 42 (9) (1994) 3157.

[5] C. Lartigue, A. Le Bail, A. Percheron-Guegan, J. Less-Common Met. 129 (1987) 65.

[6] P. Thompson, J.J. Beilly, J.M. Hasting, J. Less-Common Met. 129 (1987) 105.

[7] E. Wu, E.H. Kisi, E.M. Gray, J. Appl. Crystallogr. 31 (1998) 363.

[8] M.P. Pitt, E.M. Gray, E.H. Kisi, B.A. Hunter, J. Alloys Comp. 293–295 (1999) 118.

[9] R. Cerny, J.-M. Joubert, M. Latroche, A. Percheron-Guegan, K. Yvon, J. Appl. Crystallogr. 33 (2000) 453.

[10] E.H. Kisi, E. MacA Gray, S.J. Kennedy, J. Alloys Comp. 216 (1994) 123.

[11] B.A. Hunter, C.J. Howard, ANSTO Report — A computer program for Rietveld analysis of X-ray and neutron powder diffraction patterns, ISBN 0 642 59835 5, 1998.

[12] E. Wu, E.M. Gray, E.H. Kisi, J. Appl. Crystallogr. 31 (1998) 356.

[13] M.A. Krivoglaz, K.P. Ryaboshapka, Fiz. Met. Metalloved. 15 (1963) 18.

[14] M. Wilkens, Phys. Status Solidi (a) 2 (1970) 359.

[15] M.A. Krivoglaz, Theory of X-ray and Thermal Neutron Scattering by Real Crystals, Plenum, New York, 1969.

[16] M. Wilkens, K. Herz, H. Mughrabi, Z. Metallkd. 71 (1980) 376.